Ionics (2016) 22:2095–2102
DOI 10.1007/s11581-016-1743-9

ORIGINAL PAPER

Identification of solid electrolyte interphase formed on graphite electrode cycled in trifluoroethyl aliphatic carboxylate-based electrolytes for low-temperature lithium-ion batteries

Wei Lu[1] · **Shizhao Xiong**[2] · **Kai Xie**[3] · **Yi Pan**[3] · **Chunman Zheng**[3]

Received: 28 December 2015 / Revised: 13 May 2016 / Accepted: 14 May 2016 / Published online: 26 May 2016

Abstract Trifluoroethyl aliphatic carboxylates with different length of carbon-chain in acyl groups have been introduced into carbonate-based electrolyte as co-solvents to improve the low-temperature performance of lithium-ion batteries, both in capacity retention and lowering polarization of graphite electrode. To identify the further influence of trifluoroethyl aliphatic carboxylates on graphite electrode, the components and properties of the surface film on graphite electrode cycled in different electrolytes are investigated using Fourier transform infrared spectroscopy (FTIR), X-ray photoelectron spectroscopy (XPS), and electrochemical measurements. The IR and XPS results show that the chemical species of the solid electrolyte interphase (SEI) on graphite electrode strongly depend on the selection of co-solvent. For instance, among those species, the content of RCOOLi increases with an increasing number of carbon atoms in $RCOOCH_2CF_3$ molecule, wherein R was an alkyl with 1, 3, or 5 carbon atoms. We suggest that the thickness and components of the SEI film play a crucial role on the enhanced low-temperature performance of the lithium-ion batteries.

Keywords Fluorinated ester · Solid electrolyte interphase · Electrolytes · Low temperature · Lithium-ion batteries

✉ Shizhao Xiong
shizhao.xiong@hotmail.com; sxiong@nudt.edu.cn

[1] Institute of Applied Physics, Army Officer Academy, Hefei 230031, People's Republic of China

[2] General Logistics Department, Institute of Construction Engineering Research, Xi'an 710032, People's Republic of China

[3] College of Aerospace Science and Engineering, National University of Defense Technology, Changsha 410073, People's Republic of China

Introduction

Lithium-ion batteries have been valued in the global market of energy storage and portable devices in the past decades. Due to its advantages such as low and flat potentials (<0.25 V vs. Li^+/Li), low costs, and stable cycling performance, graphite has been employed as the overwhelming majority of negative electrodes since the commercialization of lithium-ion batteries. To match graphite-based lithium-ion batteries, conventional carbonate-based electrolytes consisting of lithium hexafluorophosphate ($LiPF_6$), ethylene carbonate (1,3-dioxacyclopentan-2-one, EC), and other linear carbonate mixed solvents are generally introduced as lithium-ion conductor between cathode and anode. In carbonate-based electrolytes, EC is crucial to form a protective solid electrolyte interphase (SEI) on the graphite anodes to restrict exfoliation since its high polarity will promote the ionization of $LiPF_6$ salt [1–3]. However, utilization of EC is accompanied with several drawbacks to the low-temperature performance of lithium ion batteries because of its high melting point, high viscosity, and low ionic conductivity at low temperature [4]. Furthermore, the SEI film formed with EC shows low Li^+ conductivity at low temperature, which limits the power and capacity of the batteries [5–7].

To overcome those issues, several strategies have been developed during the last 2 decades [4, 8–11]. Adding low melting point co-solvent is one of the most effective approaches to enhance the low-temperature performance of the lithium-ion batteries with conventional carbonate-based electrolytes [12]. Jet Propulsion Laboratory (JPL) previously reported that several battery models using their Gen 3 low-temperature electrolyte, which is the mixture of conventional carbonate-based electrolytes and ester co-solvents, showed outstanding low-temperature performances [10, 11, 13]. In these reports, K.A. Smith and his co-workers claimed that fluorinated

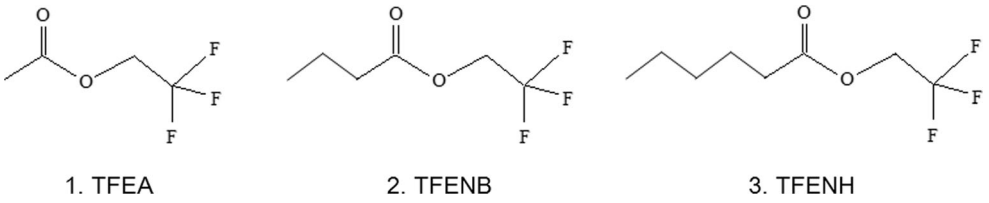

Fig. 1 Chemical structures of the fluorinated carboxylic esters investigated

aliphatic carboxylate is one of the most promising co-solvent for low-temperature electrolyte [11]. They synthesized four fluorinated esters (trifluoroethyl butyrate, trifluoroethyl acetate, ethyl trifluoroacetate and methyl pentafluoropropionate) as co-solvents and investigated the polarization behavior and the performance of batteries from room temperature to −50 °C. Their results suggested that these co-solvents are involved to formation and properties of the SEI on graphite electrode and contributing to the improved performance of batteries. Nevertheless, further details about this contribution have not been discussed yet in those literatures. The SEI on graphite electrode in several conventional carbonate-based electrolytes has been studied by several researchers during the 1990s [2, 14–18]. However, the SEI formed in the electrolyte solutions containing aliphatic carboxylates has not been fully identified. Meanwhile, the effect of chemical structure of the carboxylate co-solvent on SEI formation at low temperature also needs further investigation.

In this work, we synthesized three trifluoroethyl aliphatic carboxylates ($RCOOCH_2CF_3$) with different length of carbon-chain in their alkyl groups. Their chemical structures are shown in Fig. 1, trifluoroethyl acetate (1, TFEA), trifluoroethyl *n*-butyrate (2, TFENB), and trifluoroethyl *n*-caproate (3, TFENH). Carbonate solution 0.75 mol L^{-1} $LiPF_6$/EC + EMC (1:4, vol) is employed as the baseline electrolyte. Three modified electrolytes are obtained by mixing the three $RCOOCH_2CF_3$ co-solvents and conventional carbonate-based electrolyte, respectively. The electrochemical properties of cells using the three electrolytes are evaluated by galvanostatic charge-discharge tests and electrochemical impedance spectroscopy (EIS) at room and low temperature. Subsequently, the surface of graphite electrodes retrieved from the cycled cells is investigated by Fourier transform infrared spectra (FT-IR) and X-ray photoelectron spectroscopy (XPS).

Experimental

Synthetic process of $RCOOCH_2CF_3$ (TFEA, TFENB, and TFENH) was described in our previous work (moisture < 20 ppm) [19]. The moisture in solvents was certified by Karl-Fischer coulometric analyzer (831 KF Coulometer, Metrohm). Conventional carbonate-based electrolyte 1 mol L^{-1} $LiPF_6$/EC + EMC (1:4, vol) was acquired from Novolyte Company (moisture <10 ppm). Each ternary electrolyte was prepared by adding one $RCOOCH_2CF_3$ co-solvent to the conventional electrolyte, which can be approximately represented as 0.75 mol L^{-1} $LiPF_6$/EC + EMC + $RCOOCH_2CF_3$ (15:60:25, vol). In order to perform a reasonable comparison, 0.75 mol L^{-1} $LiPF_6$/EC + EMC (1:4, vol) binary electrolyte was obtained as the baseline electrolyte by adding mixed solvent EC/EMC (moisture < 10 ppm, Novolyte Company) in the conventional electrolyte.

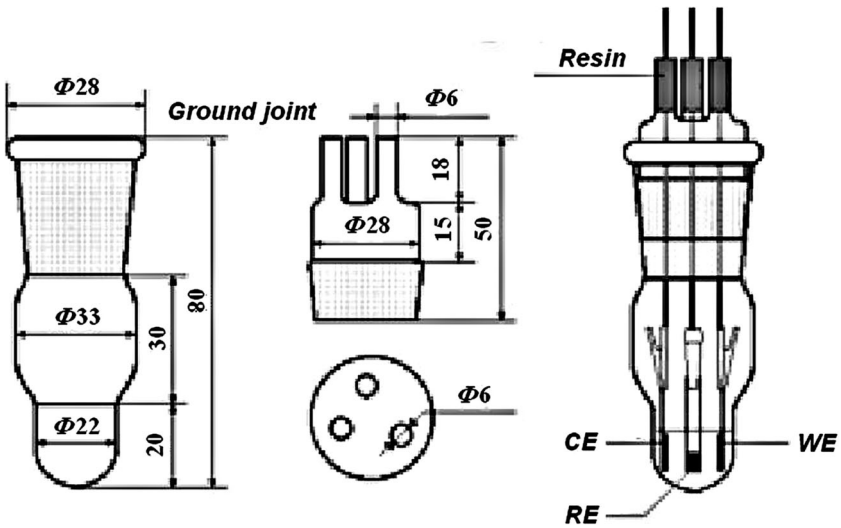

Fig. 2 Scheme of three-electrode test cell

Lowest unoccupied molecular orbital (LUMO) energies of solvent molecules were calculated using PM3 semiempirical mechanics in HYPERCHEM 7. A cell with three electrodes (lithium metal as reference electrode, platinum as working electrode and counter electrode) was prepared for electrochemical measurement. Reduction potentials of the electrolytes (1 M $LiPF_6$ in fluorinated ester) were measured using the potential linear sweep method from 0 to 3 V vs. Li^+/Li with a scan speed of 1 mV s^{-1}[20–22]. Electrochemical impedance spectroscopy (EIS) was carried out by Versa STAT MC (Princeton), using three-electrode cells like Fig. 2. Size of working electrode (WE) was 5 mm × 20 mm, and only 5 mm × 10 mm area under fluid level was covered by graphite active material. The counter electrode (CE) and reference electrode (RE) are the pure lithium foils that held the size 7 mm × 20 mm and 1 mm × 20 mm, respectively. Each cell was conducted after the SEI formation process (after five charge-discharge cycles). Collecting frequency range was from 10^5 to 0.1 Hz with an applied AC voltage of 10 mV. The polarization potential of the cells was kept at 0.1 V. The analysis of Nyquist plots was performed by Zview software.

The graphite electrode was prepared by combining 80 wt% artificial graphite (AGP-8, BTR INC.), 10 wt% acetylene black, and 10 wt% polyvinylidene fluoride (Kynar 741, Arkema Inc., USA) in *N*-methyl pyrrolidone and milling for 1 h. The electrodes were dried at 110 °C for 12 h under vacuum.

Two-electrode half-cells (CR2016) were used to evaluate the electrochemical properties of the electrolytes at room or low temperature, respectively. Lithium foil (China Energy Lithium Co., China) was used as counter-electrode. A separator (Celgard 2320) was placed between the lithium and graphite electrode. The lithium-graphite cells were assembled in a high purified argon-filled glove box. A multichannel battery testing system (LAND CT2001-A) was used to perform the charge/discharge test. All the charge-discharge tests were carried out at 0.2 C rate. Testing temperature was controlled by climate chamber. Delithiated process of graphite electrode (corresponding to charging process of the lithium-graphite cell) was tested at low temperature (−30 or −50 °C), and the cell discharged at room temperature prior to charge.

Fourier transform infrared spectra (FT-IR) of graphite electrode surfaces were conducted using Bruker Alpha spectrometer (attenuated total reflectance mode, diamond crystal) in a glove box with a resolution 2 cm^{-1} and averaging over 200 scans. For comparison, several lithium salts were synthetized by chemical route. $CH_3(CH_2)_2COOLi$, $CH_3(CH_2)_4COOLi$, and CF_3CH_2OLi were prepared by soaking lithium foil in dimethyl carbonate (DMC) with 10 % $CH_3(CH_2)_2COOH$, $CH_3(CH_2)_4COOH$ and CF_3CH_2OH for 2 h. CH_3COOLi and Li_2CO_3 were analytical-grade reagents, and their FT-IR spectra were obtained in transmittance modes (pelletized with KBr).

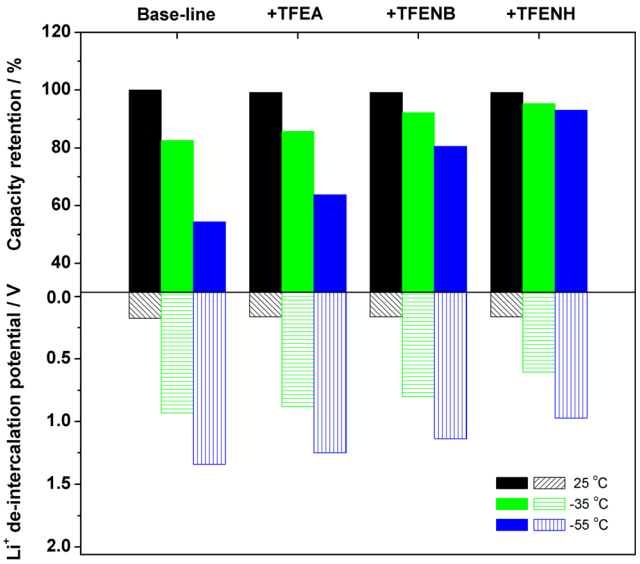

Fig. 3 Li^+ de-intercalation capacity retention and polarization potential of graphite electrode in baseline and three modified electrolytes at different temperature

The surface component of graphite electrode (cutoff voltage 0.1 V) was investigated by X-ray photoelectron spectroscopy (K-Alpha 1063, Thermo Fisher Scientific). The electrodes were sealed in argon atmosphere by a vessel and transferred into the transfer chamber without being exposed to air. C1s, F1s, Li1s, and O1s spectra were acquired using Al-K_α radiation which operated under a base pressure of 10^{-9} Torr at a power of 72 W (12 kV). Samples for surface analysis (FT-IR and XPS spectra) were retrieved from CR2016 coin cells after five charge-discharge cycles at 25 °C. The electrode samples were washed by DMC and fully dried in glove box.

Results and discussion

Here, polarization potential is defined as the voltage of lithium-graphite cell with 50 % state of charge (SOC). As shown in Fig. 3, trifluoroethyl aliphatic carboxylate could obviously increase Li^+ de-intercalation capacities and reduce polarization potential of graphite electrode at low temperature. This improvement is more effective with longer carbon-chain in the alkyl group. At −50 °C, graphite electrode with electrolyte consisting of TFENH retained over 92 % of Li^+ de-intercalation capacity at room temperature, much higher than the electrode cycling with baseline electrolyte with a value of 53 %. Meanwhile, at each testing temperature, three

electrolytes contained $RCOOCH_2CF_3$ delivered lower polarization potentials than the baseline electrolyte, which suggested lower resistance of the migration of Li^+ both in liquid and solid phases.

For further understanding of the migration of Li^+ in liquid and solid phase, electrochemical impedance spectra (EIS) of the electrodes cycling in different electrolytes were measured at different temperature [19]. The fitting results and models of the impedance spectra are shown in Figs. 4 and 5. As shown in Fig. 5, the cells using modified electrolytes show a higher R_0 at each temperature compared with the baseline electrolyte. Meanwhile, the value of R_0 shows a continuous rising with the increasing length of acyl group in the co-solvent molecular. This can be attributed to lower ionic conductivities of the electrolytes using co-solvent with long carbon-chain in acyl group. However, R_{SEI} of the cells with fluorinated ester-mixed electrolytes is lower than that with baseline electrolyte. R_{SEI} shows an exponential phase of growth adapting to the decreasing of temperature, which increases much faster than R_0. Combining with the Li^+ de-intercalating performances of the graphite electrode, it suggests that the nature of SEI layer rather than the electrolyte conductivity plays a

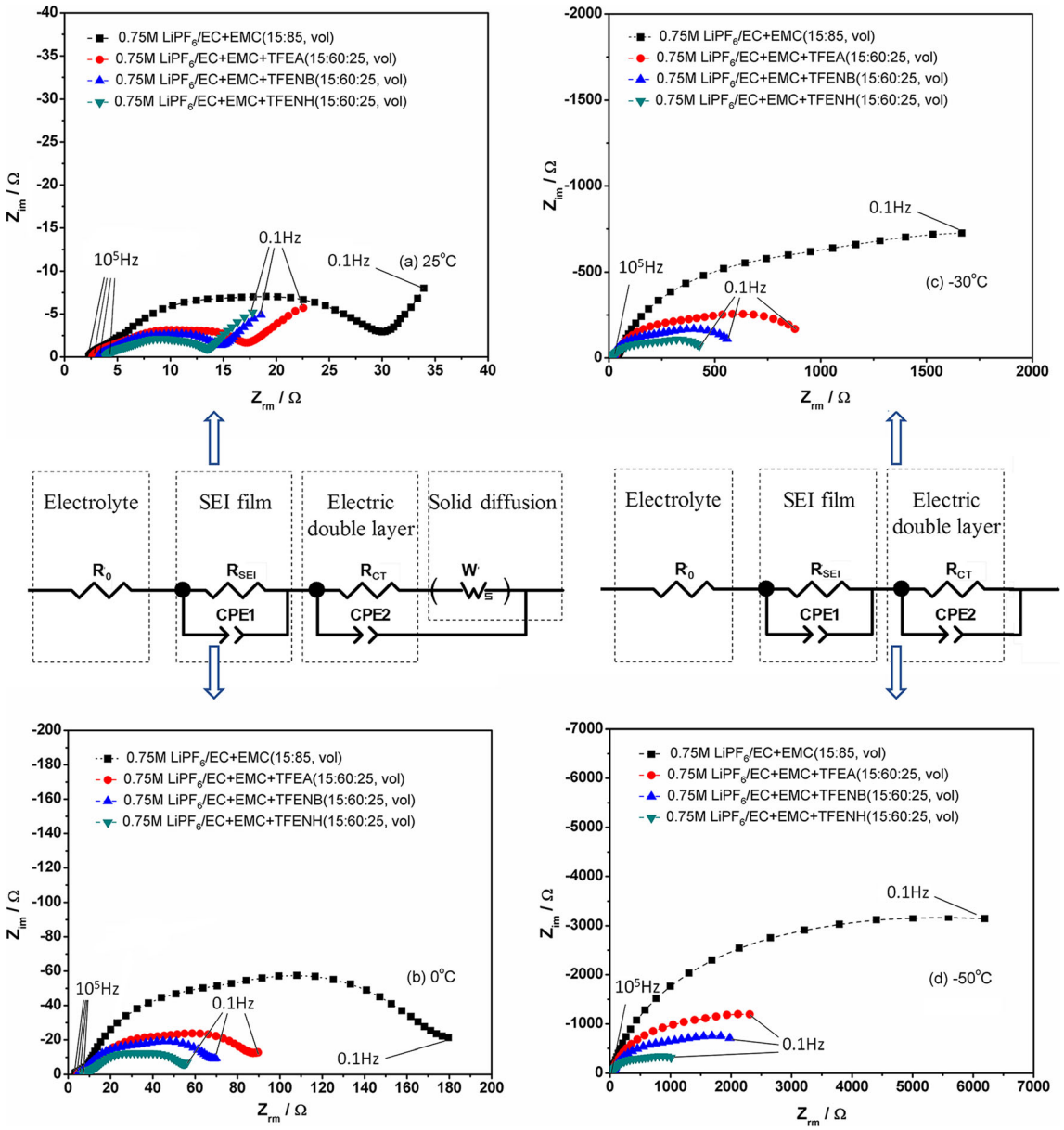

Fig. 4 Fitting results and models of the impedance spectra from symmetrical cells cycling with different electrolyte at different temperature. Best fitting line (*dash line*) and experimental point (*solid dot*)

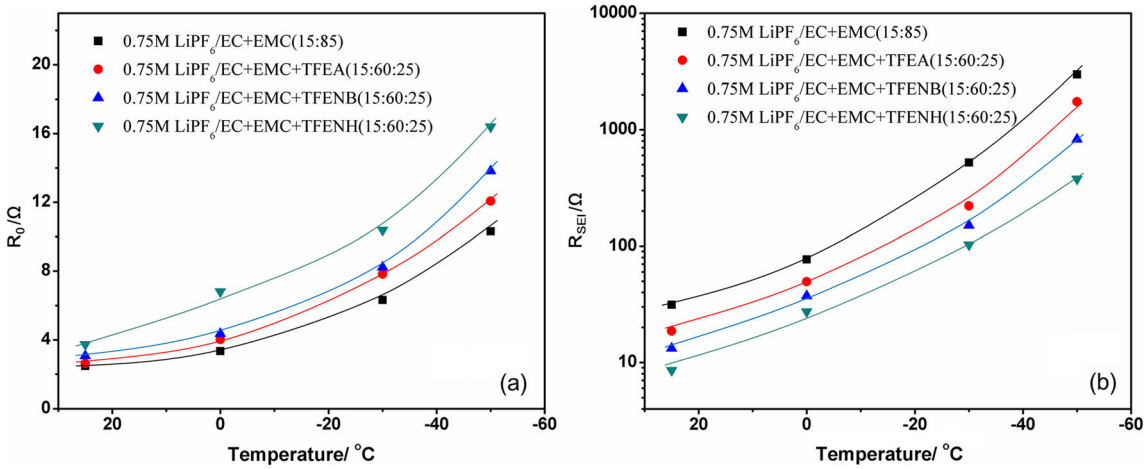

Fig. 5 Resistances R_0 and R_{SEI} as a function of temperature for the electrodes cycling with different electrolytes

significant role on the migration of Li^+ at low temperature. Particularly, TFENH with the longest acyl group might be the most promising co-solvent to form a better SEI with higher Li^+ conductivity.

To go deep into the relationship between the co-solvent and the nature of SEI on graphite electrode, the theoretical chemistry calculation and experimental Fourier transform infrared spectroscopy (FT-IR) were introduced to identify the chemical composition of SEI films. According to LUMO energies in Table 1, which are calculated using PM3 semiempirical mechanics in HYPERCHEM 7, the theoretical order of reduction stabilities could be identified as TFEA < TFENB < TFENH < EC < EMC. Based on the reduction potentials of EC, EMC and EC/EMC mixture [20], $RCOOCH_2CF_3$ also shows higher reduction potentials than the carbonates. This indicates that the reducing reaction of $RCOOCH_2CF_3$ will prior occur on negative electrode. Consequently, RCOOLi could be one of the main components in the SEI film rather than Li_2CO_3, ROLi, and lithium alkyl carbonate (ROCOOLi). Figure 6a shows the FT-IR spectra acquired from unused graphite electrode and the graphite electrodes after cycling. Typical compounds in the SEI film, such as $(CH_2OCO_2Li)_2$, $(ROCO_2Li)$ and ROLi, have been identified in the literatures [2, 14–16, 23]. For reliable comparison, Fig. 6b shows FT-IR spectra of several pure chemicals which are the possible species in SEI film formed in the electrolyte with $RCOOCH_2CF_3$ as co-solvent.

Table 1 LUMO energies and reduction potentials of the solvents

Solvents	LUMO/eV	φ_{red} (vs Li^+/Li)/V
TFEA	0.506	2.70
TFENB	0.536	2.55
TFENH	0.555	2.50
EC	1.175	1.95 [20]
EMC	1.287	2.02 [20]
EC/EMC		2.08 [20]

According to spectrum 1 and 2 in Fig. 6a, higher intensities of ATR signals are observed on the surfaces of graphite electrodes cycled in the baseline electrolyte and the electrolyte containing TFEA. With the increasing length of carbon chain in co-solvent molecule, the intensities of spectra observed from the corresponding electrode obviously decrease, as shown in spectrum 3 and 4. We suppose that the lower intensity could be due to the less reduction products on the graphite electrodes, which suggests that the decomposition of the electrolytes is suppressed with TFENB and TFENH. The assignments of the main absorption peaks in Fig. 6a are summarized in Table 2.

The decreasing intensity of peaks around 1622 and 1339 cm^{-1} indicates that the distribution of ROCOOLi gradually decreases on the surface of graphite electrodes with the increasing number of carbon atoms in $RCOOCH_2CF_3$. Meanwhile, the disappearing peak around 1455 cm^{-1} suggests that the Li_2CO_3 is gradually vanished in SEI layer. In conclusion, these results suggest that the decomposition of EC is probably restrained by the presence of $RCOOCH_2CF_3$. Particularly, the producing of Li_2CO_3, which is reported to be less conductive for Li^+, is probably suppressed adapting to the increasing carbon-chain length [26, 27].

For further investigation of the components of SEI film, X-ray photoelectron microscopy (XPS) is introduced to identify the species on the cycled graphite electrodes. Figure 7 shows the C1s, F1s, Li1s, and O1s spectra of

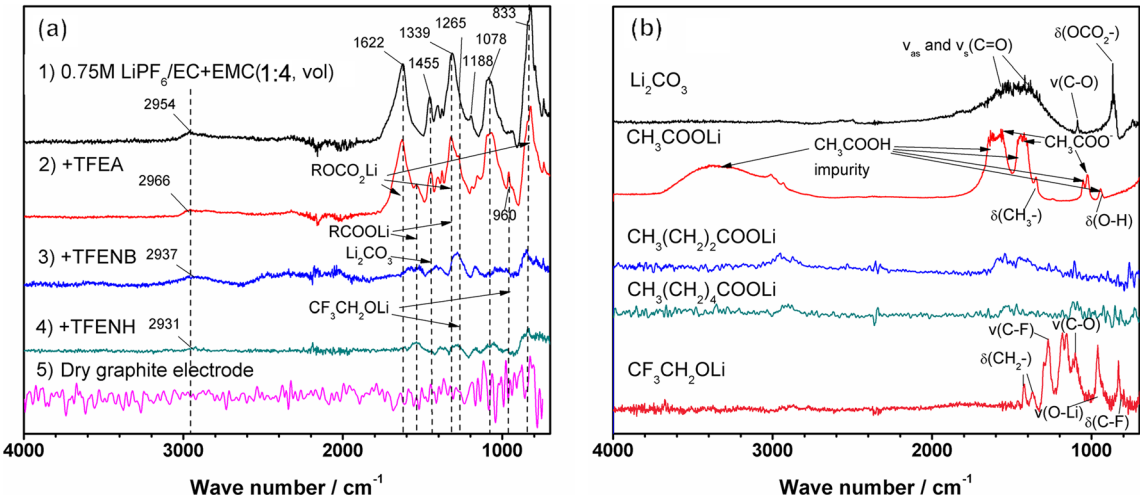

Fig. 6 **a** FT-IR spectra of the surfaces of original graphite electrodes and electrodes cycled in the four electrolytes for 5 cycles. **b** FT-IR spectra of five lithium salt for a comparison

graphite electrodes cycled in four different electrolytes at 25 °C, respectively. The assignments of the peaks in C1s spectra are listed in Table 3 [2, 16, 17, 28]. There is a possible overlap between the (R)-OCOOLi, Li_2CO_3, and the RCOOLi peaks at 290.0~290.2 eV. Two peaks of PVdF (binder of electrode) can be attributed to -(C*H_2-CF_2)$_n$- and -(CH_2-C*F_2)$_n$- which are overlapped with C-C at 285.2 eV and -C*H_2-OCOOLi at 289.2 eV. Comparing with spectrum (a) (Fig. 7a) obtained from the electrode with baseline electrolyte, the intensity of the peak at 284.5 eV significantly decreases but the peak at 285.2 eV corresponding to alkyl's C-C bonds rises accordingly after adding $RCOOCH_2CF_3$. At the same time, the peaks attributed to -COOLi around 290.0 eV are remarkably enlarged, even higher than those at 285.2 eV, as shown in spectrum (b), (c), and (d) (Fig. 7b–d). This suggests that RCOOLi, which is the decomposition product of $RCOOCH_2CF_3$, dominates the chemical species in the SEI film formed with fluorinated esters.

Furthermore, compared with -COOLi intensity of the peak attributed to -CF_3 continuously increases with the increasing number of carbon atoms in $RCOOCH_2CF_3$. This indicates the increasing decomposition of $RCOOCH_2CF_3$. As a result, there will be more RCOOLi in the SEI layer. Combining with the Li1s and O1s spectra, the content of Li_2CO_3 and ROCOOLi markedly drops down in the SEI film after adding $RCOOCH_2CF_3$ as co-solvents. It suggests that RCOOLi instead of ROCOOLi and Li_2CO_3 dominates the chemical species in the SEI film when $RCOOCH_2CF_3$ with long carbon-chain was introduced.

Peaks in the F1s spectra are assigned to LiF (685.2 eV), PVdF (687.8 eV), and CF_3CH_2OLi (689.2 eV), respectively [16, 28–30]. With the increasing length of carbon-chain, the intensity of -CF_3 peaks markedly decreases, which indicates a reducing amount of decomposed $RCOOCH_2CF_3$. These results agree with the ATR-FTIR spectra discussed in previous section.

Table 2 Summary and assignments of absorption peaks in FT-IR spectra

Wave number/cm^{-1}	Assignment		Possible species
3000~2700	ν (C-H)	In alkoxy In alkyl with long chain	(CH_3, CH_3CH_2)-OLi [2, 17] $CH_3(CH_2)_nCOOLi$ (n = 0,2,4) [24]
1632~1600	ν_{as} (C = O)	In -ROCOOLi	(CH_3, CH_3CH_2)-OCOOLi ($CH_2OCOOLi)_2$ [2, 15, 17]
1545~1531	ν (C = O)	In carboxylate	$CH_3(CH_2)_nCOOLi$ (n = 0,2,4) [24]
1455	ν (C = O)	In Li-OCO-OLi	Li_2CO_3 [15, 17, 25]
1339	ν_s (C = O)	In -ROCOOLi	(CH_3, CH_3CH_2)-OCOOLi ($CH_2OCOOLi)_2$ [2, 15, 17]
1270~1260	ν (C-F)	In fluoroalkyl	CF_3CH_2OLi [24]
970~960	δ (C-F)	In fluoroalkyl	CF_3CH_2OLi [24]
852~833	ν (P-F)	In Li_xPF_y	Li_xPF_y

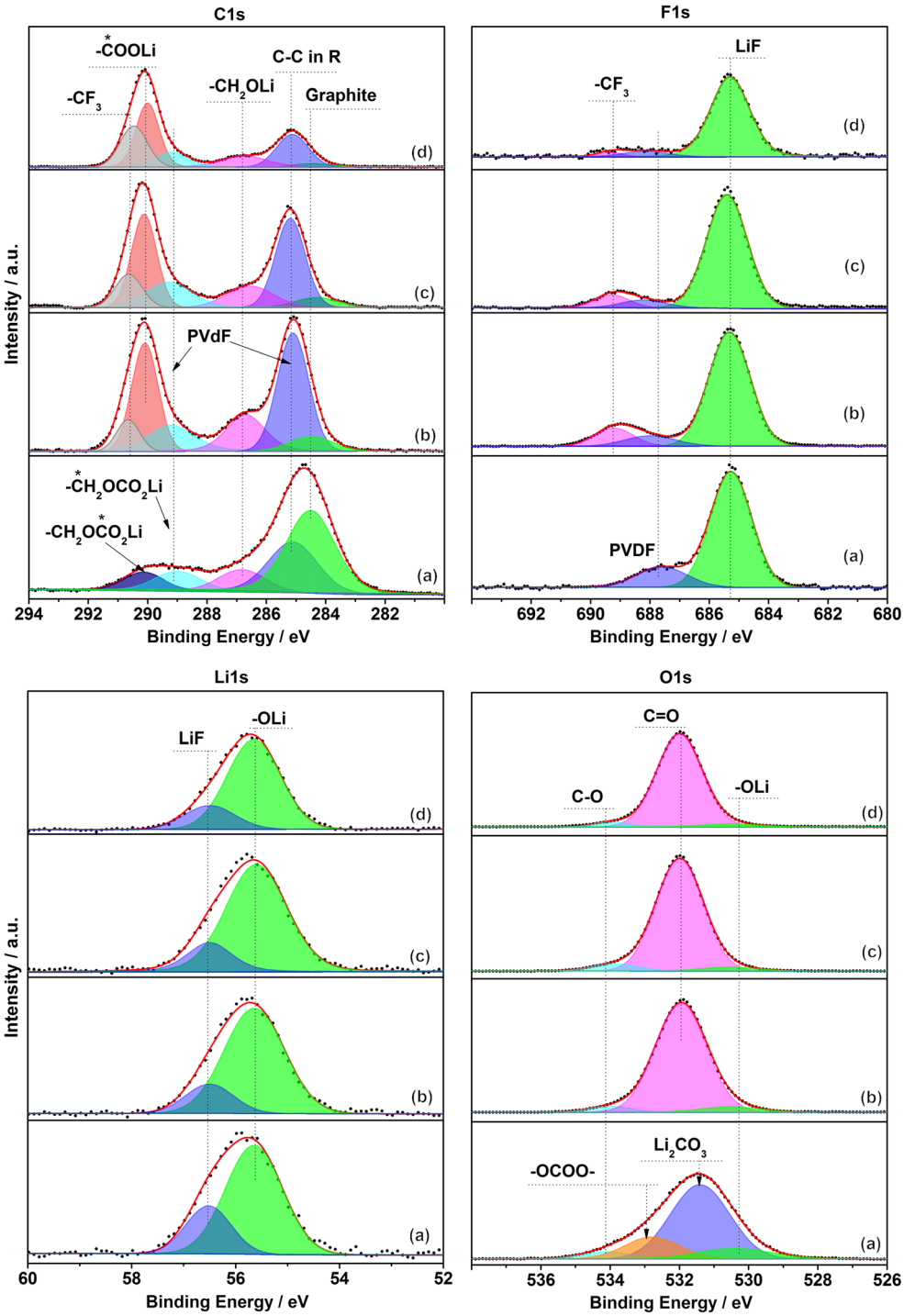

Fig. 7 XPS spectra of graphite electrodes cycled in **a** 0.75 mol L^{-1} $LiPF_6$/EC + EMC (1:4, vol), **b** 0.75 mol L^{-1} $LiPF_6$/EC + EMC + TFEA(15:60:25, vol), **c** 0.75 mol L^{-1} $LiPF_6$/EC + EMC + TFENB(15:60:25, vol), and **d** 0.75 mol L^{-1} $LiPF_6$/EC + EMC + TFENH (15:60:25, vol) electrolyte

In conclusion, the SEI film on graphite electrode cycled in baseline electrolyte mainly consists of Li_2CO_3, ROCOOLi, ROLi, and LiF [2, 15, 16]. After $RCOOCH_2CF_3$ with long carbon-chain is introduced into the electrolyte as co-solvent, CF_3CH_2OLi and R-COOLi become the main components of SEI film. We suggest that RCOOLi with long carbon-chain might be helpful to form a SEI film with higher Li^+ conductivity on the graphite electrode. However, according to the preliminary test and literature, there would be only partial solubility in carbonate-based electrolyte at room temperature when the number of carbon atoms in alkyl was above 8 [19]. Phase separation possibly occurs between co-solvent and baseline electrolyte at low temperature [31]. For this reason, among those candidates in this work, TFENH may be the

Table 3 Summary of XPS data and assignments of C1s spectra from graphite electrodes cycled in $COOCH_2CF_3$ co-solvent electrolytes

Binding energy/eV	Attribution	Possible species
284.5	Graphite	Graphite without surface layer
285.2	Alkyl	$CH_3(CH_2)_nCOOLi$ (n = 0,2,4), PVdF
286.7	R-O-Li	CH_3OLi or CH_3CH_2OLi
289.2	C*H_2-O-COOLi	(CH_3, CH_3CH_2)-OCOOLi ($CH_2OCOOLi)_2$, PVdF
290.0~290.2 eV	-COOLi	$CH_3(CH_2)_nCOOLi$ (n = 0,2,4)
	-O-COOLi	Li_2CO_3, (CH_3, CH_3CH_2)-OCOOLi ($CH_2OCOOLi)_2$
290.5	-CF_3	CF_3CH_2OLi

most suitable co-solvent for low-temperature carbonate-based electrolyte.

Conclusions

Carbonate-based electrolytes with trifluoroethyl aliphatic carboxylate as co-solvent were systematically investigated for low-temperature lithium-ion batteries. We found that the cells using these co-solvents deliver higher Li^+ intercalation capacities than baseline electrolyte at low temperature without compromise to the performance at room temperature. Especially, in 0.75 mol L^{-1} $LiPF_6$/EC + EMC + TFENH (15:60:25, vol) electrolyte, the retained capacity of the cell maintains about 92 % at −50 °C, much higher than the one using baseline electrolyte with a value of 53 %. The results of FT-IR and XPS spectra show that Li_2CO_3 and ROCOOLi instead of RCOOLi dominate the chemical components in the SEI film with the increasing number of the carbon atoms in $RCOOCH_2CF_3$ molecule. This film plays an important role on the improvement of low-temperature performances for the full lithium-ion batteries, due to the lower resistance of Li^+. TFENH may be the most suitable co-solvent for low-temperature carbonate-based electrolyte.

References

1. Chung G, Kim H, Yu S, Jun S, Choi J, Kim M (2000) J Electrochem Soc 147:4391
2. Aurbach D, Markovsky B, Weissman I, Levi E, Ein-Eli Y (1999) Electrochim Acta 45:67
3. Xu K, Lam Y, Zhang S, Jow T, Curtis T (2007) J Phys Chem C 111: 7411
4. Smart MC, Ratnakumar BV, Surampudi S (1999) J Electrochem Soc 146:486
5. Huang CK, Sakamoto JS, Wolfenstine J, Surampudi S (2000) J Electrochem Soc 147:2893
6. Contestabile M, Morselli M, Paraventi R, Neat RJ (2003) J Power Sources 119–121:943
7. Zhang SS (2006) J Power Sources 162:1379
8. Smart MC, Ratnakumar BV, Whitcanack LD, Chin KB, Surampudi S, Croft H, Tice D, Staniewicz R (2003) J Power Sources 119–121: 349
9. Plichta EJ, Hendrickson M, Thompson R, Au G, Behl WK, Smart MC, Ratnakumar BV, Surampudi S (2001) J Power Sources 94:160
10. Smart MC, Ratnakumar BV, Ryan-Mowrey VS, Surampudi S, Prakash GKS, Hu J, Cheung I (2003) J Power Sources 119–121: 359
11. Smith KA, Smart MC, Prakash GKS, Ratnakumar BV (2008) ECS Trans 11:91
12. Herreyre S, Huchet O, Barusseau S, Perton F, Bodet JM, Biensan P (2001) J Power Sources 97–98:576
13. Smart MC, Whitacre JF, Ratnakumar BV, Amine K (2007) J Power Sources 168:501
14. Aurbach D, Zaban A, Gofer Y, Ely YE, Weissman I, Chusid O, Abramson O (1995) J Power Sources 54:76
15. Aurbach D, Zaban A, Ein-Eli Y, Weissman I, Chusid B, Markovsky M, Levi E, Levi A, Schechter E, Granot Y (1997) J Power Sources 68:91
16. Peled E, Golodnitsky D, Menachem C, BarTow D (1998) J Electrochem Soc 145:3482
17. Aurbach D, Gamolsky K, Markovsky B, Gofer Y, Schmidt M, Heider U (2002) Electrochim Acta 47:1423
18. Sasaki T, Abe T, Iriyama Y, Inaba M, Ogumi Z (2005) J Electrochem Soc 152:A2046
19. Lu W, Xie K, Chen Z, Pan Y, Zheng C (2014) J Fluor Chem 161: 110
20. Xu K (2009) Electrolytes: overview, secondary batteries – lithium rechargeable systems. Elsevier, London, p 51-53
21. Ue M (2009) Electrolytes: nonaqueous, secondary batteries—lithium rechargeable systems. Elsevier, London, p 72-75
22. Hayashi K, Nemoto Y, Tobishima S, Yamaki J (1999) Electrochim Acta 44:2337
23. Aurbach D, Zinigrad E, Cohen Y, Teller H (2002) Solid State Ionics 148:405
24. Ke Y, Dong H (1998) Handbook of analytical chemistry (second edition)-spectroscopic analysis. Chemical Industry Press, Beijing, p 101-109
25. Aurbach D, Gnanaraj JS, Geissler W, Schmidt M (2004) J Electrochem Soc 151:A23
26. Chen YC, Ouyang CY, Song LJ, Sun ZL (2011) J Phys Chem C 115:7044
27. Shi S, Lu P, Liu Z, Qi Y, Hector LG, Li H, Harris SJ (2012) J Am Chem Soc 134:15476
28. Nie M, Abraham DP, Chen Y, Bose A, Lucht BL (2013) J Phys Chem C 117:13403
29. Sato K, Zhao L, Okada S, Yamaki J (2011) J Power Sources 196: 5617
30. Wu B, Ren Y, Mu D, Zhang C, Liu X, Wu F (2013) Int J Electrochem Sci 8:8502
31. Zheng H (2006) Lithium-ion batteries electrolyte. Chemical Industry Press, Beijing, p 260-265